

URANUS: Radio Frequency Tracking, Classification and Identification of Unmanned Aircraft Vehicles

Domenico Lofu^{a,b}, Pietro Tedeschi^c, Tommaso Di Noia^a, Eugenio Di Sciascio^a

^a*Dept. of Electrical and Information Engineering (DEI), Politecnico di Bari, Bari (Italy),
{domenico.lofu, tommaso.dinoia, eugenio.disciascio}@poliba.it*

^b*Innovation Lab, Exprivia S.p.A., Molfetta (Italy)
domenico.lofu@exprivia.com*

^c*Technology Innovation Institute, Autonomous Robotics Research Center, Abu Dhabi,
United Arab Emirates
pietro.tedeschi@tii.ae*

Abstract

Safety and security issues for Critical Infrastructures (CI) are growing as attackers increasingly adopt drones as an attack vector flying in sensitive airspace, such as airports, military bases, city centres, and crowded places. The rapid proliferation of drones for merchandise, shipping recreations activities, and other commercial applications poses severe concerns on the CI operators due to the violations and the invasions of the restricted airspaces. A cost-effective framework is needed to detect, classify and identify the presence of drones in such cases. In this paper, we demonstrate that CI operators can detect, classify and identify timely and efficiently drones (multi-copter and fixed-wings) invading no-drone zones, with an inexpensive RF-based detection framework named URANUS. Our experiments show that by using Random Forest classifier, we achieved a classification accuracy of 93.4% in the classification of one or multiple specific drones. The tracking performance achieves an accuracy with an average of MAE=0.3650, MSE=0.9254 and $R^2 = 0.7502$. Our framework has been released as open-source, to enable the community to verify our findings and use URANUS as a ready-to-use basis for further analysis.

Keywords: Drone Identification, Security, Cyber Physical Systems, ML for Drone Detection.

1. Introduction

In the last years Unmanned Aerial Vehicleless (UAVs), commonly known as *drones* have become a crucial technology for several types of applications such as environmental monitoring [1, 2, 3], smart grids control [4], crime prevention [5, 6], smart cities management [7], and the military field [8]. According to authoritative marketing research industries, the autonomous vehicles market is estimated to be 0.5 million units in 2025 and is projected to reach 6.9 million units by 2030. The global drone logistics & transportation market accounted for US\$ 24.58 million in 2018 is expected to grow at a CAGR of 60.6% over the forecast period 2019-2027, to account for US\$ 1,626.98 million in 2027. Factors including increasing developments in the e-commerce sector and rising acceptance owing to various benefits offered are significantly driving the global drone logistics & transportation market.

Most commercial drones are autonomous (vehicles) or remotely controlled by users vehicles via the standard Wi-Fi frequency bands, i.e. 2.4 GHz and 5.0 GHz. They can be programmed to execute tasks that span from object tracking, and delivery, to committing illegal activities such as privacy violations, destroying critical infrastructures and harming public safety during crowded events [9]. Given the above threats, in the last few years, several counter-measures based on audio, video, thermal and Radio-Frequency (RF) signals have been exploited for drone detection, identification and tracking. However, the performance of these systems can be affected when the surrounding environment is impaired (e.g. weather conditions, noise, low light visibility). Indeed, most of the critical infrastructures adopt Radio-Frequency (RF)/Direction Findings (DF) and kinematics radar sensors that detect all types of drones by analyzing the reflected signals and comparing them to a database for drone characterization. As a consequence of the high number of unauthorized UAVs operating in the skies, it is crucial to deploy a system framework to identify, classify and track timely, malicious UAVs by leveraging the data provided by radar sensors.

Contribution. To address the above introduced challenging scenario, in this paper we propose URANUS. It is a system specifically designed to *track*, *classify* and *identify* Unmanned Aircraft Vehicles (UAS), as they fly within a defined area, from data provided by certain types of sensors. Our work, performed over a real dataset of UAVs flights provided by North Atlantic Treaty Organization (NATO) [10], demonstrates that it is possible to:

- identify, classify and track one or more drones in flight;
- classify fixed wing and multi-copter drones;
- analyze both RF/DF and kinematics sensors to detect aerial vehicles in critical infrastructures.

We provide a machine learning framework, namely URANUS, based on Random Forest that reaches a classification accuracy of 93.4% in the detection, classification and tracking of one or multiple specific drones. Our prototype implementation, available online as opens source code [11], adopts popular libraries and tools such as *scikit-learn*, *pandas*, and *scipy*.

Roadmap. The rest of the paper is organized as follows: Section 2 reviews the related work. Section 3 highlights the reference scenarios and the adversary model. Section 4 provides the details of URANUS. Section 5 reports the performance assessment of URANUS. Section 6 highlight conclusions and future research directions.

2. Related Work

In this section, we review the state of the art on the Radio Frequency (RF) machine learning and deep learning approaches adopted to detect, identify and track drones. Our analysis are summarized in Table 1 with a model performance evaluation.

For instance, Al-Sa’d *et al.* [12] collected, analysed, and recorded raw RF signals from several types of drones in different states. Further more, they leveraged a deep learning technique to detect and identify malicious drones and

Table 1: Comparison and overview of related contributions on drones RF identification, classification and tracking using Machine Learning and Deep Learning techniques. A ✓ symbol indicates the fulfillment of a particular feature, a ✕ symbol denotes the miss of the feature or that the feature is not applicable.

Ref.	Analysis on Dataset	Identification and Classification	ML/DL Model	Model Performance Evaluation	Multiple Drone Detection	Fixed-wing Drone Detection	Path Tracking	Open Source Code
[12]	✕	✓	DNN	Accuracy 99.7%	✓	✕	✕	✓
[13]	✕	✓	YOLO-lite	F1-Score 97%	✕	✕	✕	✕
[14]	✓	✓	CNN	Accuracy 99.7%	✕	✕	✕	✕
[15]	✓	✓	1D-CNN	Accuracy 87,4%	✕	✕	✕	✕
[16]	✓	✓	XGBoost	Accuracy 99.96%	✕	✕	✕	✕
[17]	✓	✓	FC-DNN	Accuracy 97.3%	✓	✕	✕	✕
[18]	✓	✓	DRNN	Accuracy 99%	✓	✕	✕	✕
[19]	✓	✓	KNN and XG-Boost	Accuracy 99%	✕	✕	✕	✕
[20]	✕	✓	KNN, SVM and RandF	Accuracy 100%	✕	✕	✕	✕
URANUS	✓	✓	RandF	Accuracy 93.4%	✓	✓	✓	✓

their flight mode. The authors designed three Deep Neural Networks (DNNs) to (i) detect the drone, (ii) detect the drone and recognize its type and (iii) detect the drone, and recognize its type and its state. The authors do not consider fixed-wing drones and they do not perform any path tracking operation.

Basak *et al.* [13] focused on the development of an (i) RF drone signal detection, a (ii) spectrum localization and a (iii) drone classification by using a two-stage technique. In the first stage, they adopt the Goodness-of-Fit (GoF) sensing for the drone detection and the Deep Recurrent Neural Network (DRNN) framework for the drone classification. In the second stage, they use the You Only Look Once - lite (YOLO-lite) framework to perform the combined drone RF signal detection, spectrum localization, and drone classification. However, neither multiple detections of drones nor trajectory tracking on a map are considered.

Al-Emadi *et al.* [14] proposed a real-time RF drone detection and identification framework to inspect the radio spectrum between the drone and its controller. The solution adopts a Convolutional Neural Network (CNN) to train and test an RF dataset released by [12]. The experimental results show the effectiveness and feasibility of using RF signals in combination with a CNN to detect and identify a drone. The proposed solution achieves an F1 score of 99.7% for drone identification. Nevertheless, the authors do not consider fixed-wing drones and drone path tracking operations.

Allahham *et al.* [15] investigated deep learning techniques to perform (i) drone detection, (ii) drone detection and type identification, and (iii) drone detection, type and state identification by using a three multi-channel 1-dimensional CNN. The dataset adopted in the experiments is *Drone RF* dataset [21]. The performance for (i) shows an average accuracy of 100%, while (ii) has an accuracy of 94.6%, and, finally, the last one (iii) presents an accuracy of 87.4%.

The authors in [16] developed an RF machine-learning drone detection and identification system by analyzing the low-band RF signals emitted by the flight controller. They proposed three machine learning models based on eXtreme Gradient Boosting (XGBoost) algorithm to detect and identify (i) the presence

of a drone, (ii) the presence of a drone and type, and (iii) the presence of a drone, type and the operational mode. The accuracy achieved by the three models is 99.96%, 90.73%, and 70.09%, respectively. It results that the higher the model complexity, the lower the model accuracy. This implies the low effectiveness of using the frequency components of a signal as a signature to detect the activities performed by drones. Also in this case, trajectory tracking on a map is not considered.

Sazdić-Jotić *et al.* [17] proposed RF detection and identification algorithms to detect and identify a single or multiple drones. They built an RF dataset by considering scenarios with (i) a single drone, (ii) two drones, and (iii) three drones. They detect and identify a single drone with an accuracy of 99.8% and 96.1%, respectively, while the results of detecting multiple drones show an average accuracy of 97.3%. The deep learning algorithms used are mainly Fully Connected Deep Neural Networks (FC-DNN). Although the approach achieves good performance, the authors do not consider path tracking.

The authors in [18] presented a DRNN that classifies different drone signals in single-drone and multiple drone scenarios. The authors built an RF dataset with nine commercial drone types, and further, they evaluated the proposed model in Additive white Gaussian noise (AWGN) and multipath conditions. The model achieved roughly 99% classification accuracy for single and simultaneous multi-drone scenarios. However, the described approach does not take into account drone path tracking and fixed-wing drones.

Ibrahim *et al.* [19] presented an UAV identification and hierarchical detection approach by leveraging an ensemble learning based on K-Nearest Neighbor (KNN) and XGBoost. The proposed solution allows to (i) check the availability of a UAV, (ii) specify the type of the UAV, and then (iii) determine the flight mode of the detected UAV. This approach reaches a classification accuracy of around the 99%. However, the authors do not consider drone path tracking.

Wei *et al.* [20], proposed a drone detection and identification system based on WiFi signals and high-frequency RF fingerprints. The system (i) performs UAV detection, (ii) extracts the features Fractal Dimension (FD), (iii) Axially

Integrated Bispectra (AIB) and Square Integrated Bispectra (SIB) (iii) adopts the Principal Component Analysis (PCA) algorithm for the feature dimensionality reduction, and (iv) applies the Neighborhood Component Analysis (NCA) algorithm for metric learning. Finally, the authors test KNN, Support Vector Machine (SVM), and Random Forest (RandF) to identify UAVs. They verified their model in two different scenarios, i.e., indoor with a Signal-to-Noise Ratio (SNR) of 10 dB and outdoor with a SNR of 3 dB. In the indoor scenario, the average identification accuracy of FD, AIB, SIB is 100%, 97.23%, and 96.11% respectively. In the outdoor scenario, the identification accuracy of same features is 100%, 95.00%, and 93.50% respectively. The drone trajectory tracking is not considered by the authors.

To sum up, the discussion above confirms that despite there are several contributions to the state-of-the-art, none of them analyze and evaluate the proposed techniques on both fixed-wing and multi-copter drones for the (i) detection, (ii) classification and (iii) simultaneous tracking, as well as the drone path tracking. Such constraints make previous solutions unsuitable for this problem and call for new domain-specific approaches.

3. Reference Scenarios and Adversarial Model

This section introduces the scenario and the adversarial model considered in our work. Specifically, section 3.1 depicts the system model and describe the assumption, while section 3.2 describes the adversary model.

3.1. System Model and Assumptions

The scenario assumed in this work is depicted in figure 1. We consider to tackle the problem of detecting, classifying and tracking one or multiple drones (multi-copter or fixed wing) in a No-Drone Zone [22]. It is worth noticing that we refer to the scenario described by NATO [10].

We define here after the main components in our scenario:

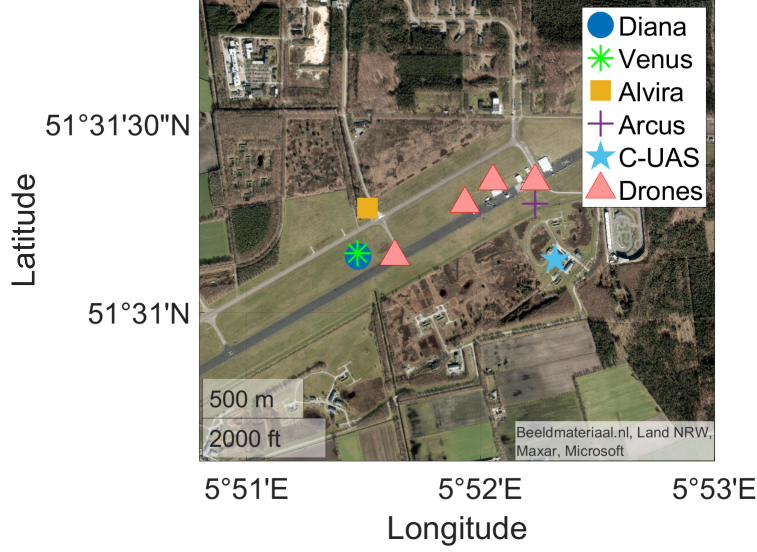


Figure 1: Scenario assumed in this work.

- **No-Drone Zone (NDZ).** The Federal Aviation Administration (FAA) introduced the term NDZ to describe an area that does not allow to operate by using a drone or unmanned aircraft system. Examples of NDZ areas are airports, restricted airspaces, government agencies or also temporary flight restrictions areas such as sport events, presidential movements, and security-sensitive areas.
- **Drone.** The drone(s) assumed in this scenario are classified with the features reported in Table 2. Each drone is characterized by the commercial name and a code field, a unique identifier assigned during the drone configuration phase. The airframe represents the type of drone, i.e. a multi-copter or a fixed-wing drone, the weight specifies the maximum weight of the drone, and velocity indicates the maximum speed of the drone. Radar cross-section (RCS) or radar signature measures how much energy the drone reflects towards a radar, i.e. the area seen by a

radar. Frame Cross Section Frontal (FCSF) defines a frame of the frontal measurement of the cross-section.

Table 2: Classification and characteristics of the drones.

Drone Name	Airframe	Weight [<i>kg</i>]	Max Velocity [<i>m/s</i>]	RCS [<i>m</i> ²]	FCSF [<i>m</i> ²]
DJI Mavic Pro	Multi- copter	1	20	0.01	0.02
DJI Mavic 2	Multi- copter	1	20	0.01	0.02
DJI Phantom 4 Pro	Multi- copter	1	20	0.01	0.02
Parrot Disco	Fixed wing	1	20	0.005	0.1

- **RF-DF/Radar Sensor Network.** The No-Drone Zone is monitored by two Radio Frequency (RF)/Direction Finding (DF) sensors namely Diana and Venus, and two radar sensors namely Arcus and Alvira. From one side, Diana and Venus (fictitious names) sensors acquire data such as time-of-arrival (timestamp), Receiving Signal Strength (RSS) and beamforming to localize the target. Diana adopts a linear array antenna to estimate the bearing of an intercept; it only reports detections in a 180° sector even if the target is located in the opposite sector. Venus uses a circular array antenna with no bearing ambiguity and provides no range information. On the other side, Arcus and Alvira (fictitious names) sensors are 2D radar and 3D radar, respectively. These sensors provide crucial information such as latitude, longitude, altitude, timestamp, as well as the bearing and range of the drone during the flight. Table 3 summarizes the name, the type and the sensor location (latitude and longitude coordinates).

Table 3: Details on the sensor network deployment.

Sensor Name	Sensor Type	Sensor Lat.	Sensor Lon.
Diana	RF/DF	51.51913°	5.85795°
Venus	RF/DF	51.51927°	5.85791°
Alvira	Radar	51.52126°	5.85860°
Arcus	Radar	51.52147°	5.87056°

- **Counter Unmanned Aerial System (C-UAS).** It is a central server unit adopted to collect and process (via URANUS) the data generated by the sensor network. The system is used to detect, identify and track the presence of any unauthorized or malicious drone in the No-Drone Zone.

As mentioned above, our scenario assumes the presence of a Counter Unmanned Aerial System (C-UAS) operator in a NDZ, e.g., the one controlling a generic critical infrastructure. Such operators are interested in monitoring the critical infrastructure, looking for malicious and unauthorized UAVs approaching a sensitive area. To this aim, the operators adopt an RF-DF/Radar sensor network to capture crucial information in the monitored area to identify, classify and track the owner of the UAV. In this paper, we consider three scenarios as follows:

- **Scenario 1.** In this scenario, we assume a single UAV (multi-copter) is flying in the NDZ.
- **Scenario 2.** In this scenario, we assume two UAVs (multi-copter) are flying in the NDZ.
- **Scenario 3.** In this scenario, we assume one UAV (fixed-wing) is flying in the NDZ.

We highlight that the three scenarios described above are only a reference for the considered dataset, and our research can be directly applicable also to other use-cases such as surveillance towers around critical infrastructures, military bases, ports, and airports.

3.2. Adversary Model

In all the scenarios, we assume that an adversary \mathcal{E} has the capabilities to radio-control a single drone or a swarm of drones, and it is interested to reach a target inside a NDZ. The aims of the adversary can be manifold, e.g., violating the privacy of the area by recording video and/or taking photos of a sensitive area, using it as a bomb in critical infrastructures such as airports, oil&gas industries, nuclear power plants, water treatment facilities, ports, telecommunication networks, or to threat people safety by carrying explosives or radioactive materials or colliding with airplanes during the take-off and landing procedures. Moreover, the adversary \mathcal{E} can control a drone in several ways: (i) through a wireless remote controller, (ii) remotely via Internet (i.e. the drone supports embedded SIM, standard SIM and cellular Long Term Evolution (LTE) or 5G technology), (iii) by pre-programing it through waypoints to enable the autonomous flight. Conversely, we assume that the drones are broadcasting data (for several purposes) via the onboard radio transmitter for the whole flight [23].

4. The URANUS Framework

In this section we focus our discussion on our experimental campaign. We start describing the datasets we used for our experiments and then we move to the Radio Frequency analysis (RCS and drone operating frequency) over the dataset. We then show an example scenario to better describe the adopted techniques for feature selection and classification. Finally, we detail the implementation of URANUS. Section 4.1 describes the dataset adopted for these experiments. Section 4.2 introduces the Radio Frequency analysis (RCS and drone operating frequency) over the dataset. Section 4.3 reports the analysis about the drone movement(s) for an example scenario. Section 4.4 describes the data pre-processing and the feature selection operations over the dataset. Section 4.5 motivates the adoption of the Random Forest algorithm, while Section 4.6 reports the implementation details of URANUS.

4.1. Dataset Organization

The dataset adopted in this work (available at [10]) is organized into a training set and test set as shown in Table 4. For each scenario and each drone in flight as well, the training set folder stores the RF readings of the sensors Alvira, Arcus, Diana and Venus, and the drone log files; the test set stores only the RF readings of the aforementioned sensors.

Table 4: Description of the organization of the dataset folders used in the experiments.

Training Set	Test Set
Scenario 1.1	Scenario 1.2a
Scenario 1.2b	Scenario 1.4a
Scenario 1.3	Scenario 3.1
Scenario 1.4	Scenario 3.1a
Scenario 2.1	Scenario 3.3
Scenario 2.2	Scenario 3.4.text
Scenario 3.Parrot.a	Scenario 3.Parrot.d

It is worth noticing that the drone log file keeps track of its parameters such as the latitude, longitude, speed, altitude, and drone type. Further, we highlight that the RF features such as the RCS, RF frequency, and the data of drone log files are stored along with the UNIX timestamp. Indeed, this latter is adopted as an index of each data frame to merge and correlate the RF sensors’ readings, and the drone data logs. Therefore, we decided to use these data to train our machine learning model to *track* the drone position, *classify* the drone type (i.e. multi-copter or fixed-wing) and *identify* the drone model.

4.2. Radio Frequency Analysis

In this subsection, we analyze the two most important features from the RF perspective, i.e, the drone RCS, and the drone operating frequency channel. Radar cross-section or radar signature indicates if an object can be easily detected from the radar. The larger it is, the easier it will be the detection. The

factors that influence the RCS span from the material with which the object is made to the size of the object. Unfortunately, the authors of the dataset do not specify the frequency band of the RCS data. However, it is worth noticing that the RCS varies with observation angles and slightly fluctuates with frequency. Indeed, in this case, we consider the RCS signature as a random variable characterized by the associated Probability Density Function (PDF). Figure 2 shows the PDFs for a Mavic Pro, Mavic 2, Parrot and the Phantom 4 Pro. All of them follow a Normal distribution. The maximum likelihoods are

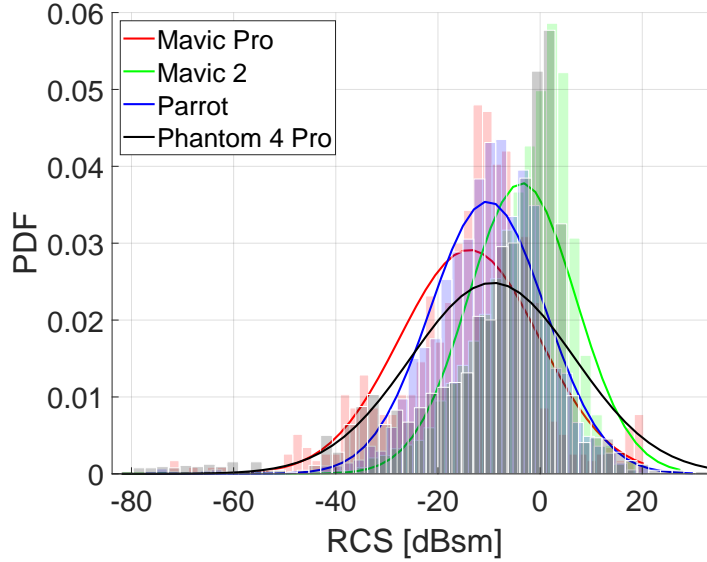


Figure 2: Probability distribution function associated with the measured RCSs for the four drone models.

≈ -14.05 dBsm for a Mavic Pro, ≈ -3.11 dBsm for a Mavic 2, ≈ -10.82 dBsm, and ≈ -8.55 dBsm for the Phantom 4 Pro. Finally, we evaluated the maximum likelihood of the drone operating frequency. From the dataset, we obtain that with 44% of probability we classify a Mavic Pro on 2,4065 MHz, with 36% for a Mavic 2 on 2,4165, with the 100% for a Parrot on 2,4400 MHz, and with 38% for a Phantom 4 Pro on 2,4715 MHz.

4.3. Path Tracking Analysis

In the following, we report an example about the analysis of the drone movements in the Scenario 1.1. We remark that we performed this analysis for all the dataset provided by NATO [10]. As shown in Figure 3, we analyzed a fly-

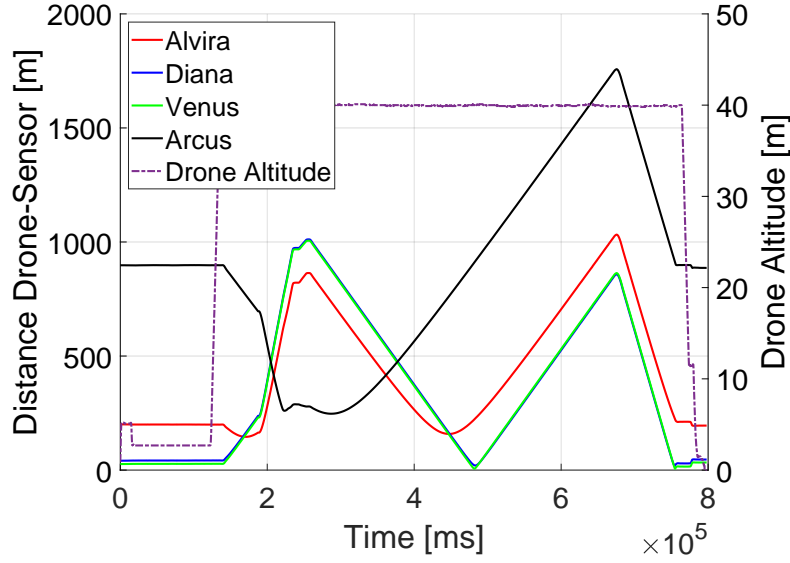


Figure 3: Distance Drone-Sensor(s) and Drone Altitude over the time t in Scenario 1.1. The figure reports an analysis about the drone movements.

ing window of 797,983 ms by computing the distance between the drone and each radar sensor, and its altitude during the time t . We observe that in this case, the drone reaches a maximum altitude of 40 meters and that the distance from each sensor fluctuates during the time. However, we repeated this analysis over all the dataset scenarios to identify crucial features of flying patterns and distinguish a drone from another flying object.

4.4. Data Pre-processing and Feature Selection

In this subsection, we present the pre-processing tasks to get a cleaned data that allowed us to improve the accuracy for the proposed classifier. Further

more, we detail the feature selection process.

1. **Missing Values Analysis.** The problem related to missing value in a dataset is common during the data collection process. Our analysis leverages visualization techniques:

- *Heatmaps*: it shows the missing data for each feature of the dataset;
- *Histogram*: it shows the distribution of the the missing values for the dataset's features;
- *Percentage List*: it shows the percentage of missing values for each feature in the given dataset.

In accordance with Rubin [24] we categorized the missing data as i) Missing completely at Random (MCAR), ii) Missing at Random (MAR), and iii) Missing not at Random (MNAR).

2. **Irregular Values Analysis.** In this phase, we also analyzed the errors that may occur during the data sensor acquisition. These anomalies, namely *outliers*, should be dropped due to the fact that environmental conditions could negatively affect the performance during the RF acquisition phase. We adopted the Inter Quartile Range (IQR) method [25].
3. **One Hot Encoding.** Is a technique to converting categorical data variables into binary values and make the training data more useful for the machine learning model. In details, categorical variables are replaced with 1 if an observation is scored, 0 [26].

Feature Selection. In order get a better performances for the classification task, we performed a feature selection by using the one-way Analysis of Variance (ANOVA) tool. Indeed, it was fitted to test the relationship among the sensor features and the feature target. In our case, for Alvira and Arcus (kinematic sensors), we considered features such as latitude, longitude, speed, and flight altitude. For Diana and Venus (RF sensors), we selected several features like the drone type, RCS, SNR.

4.5. Machine Learning Model(s) Discussion

In this section, we present and comment on the choice of using Random Forest Regressor and Classifier in this work.

Regression Models Comparison. In order to determine the best regression model to predict variables such as latitude, longitude, speed and altitude, we analyzed the following regression models:

- *K-Neighbors regressor* [27]
- *Stochastic Gradient Descent regressor* [28]
- *Gradient Boosting regressor* [29]
- *Random Forest regressor* [30]

We trained the machine learning algorithms on the drone’s latitude, longitude, speed and altitude, by defining the drone speed as the target variable. To evaluate the regression models, we evaluated their accuracy. Indeed, for the *KNeighbors regressor* we estimated an average accuracy between ≈ 0.55 and ≈ 0.64 . We get better results with the *SGD regressor* and *Gradient Boosting regressor* with an average accuracy for both models between ≈ 0.61 and ≈ 0.74 . Finally, with the *Random Forest* regressor we obtain an overall average accuracy between ≈ 0.76 and ≈ 0.82 . We selected the Random Forest not only for the higher accuracy, but we computed for each model the Mean Absolute Error (MAE) and Mean Squared Error (MSE) as described in Section 5.1.

Classification Models Comparison. In order to determine the best classification model to predict the drone type, we analyzed the following models:

- *K-Neighbors Classifier* [27]
- *Support Vector Classifier* [31]
- *Multi-layer Perceptron Classifier* [32]
- *Random Forest Classifier* [30].

In order to evaluate the classification models, we studied the accuracy and the F1 score metrics as described in Section 5.1. It is worth noticing that with the *KNeighbors Classifier*, we have an accuracy of ≈ 0.77 and the F1 score of ≈ 0.8 . With the *SVC* and *MLP Classifier*, we reach an average accuracy of ≈ 0.51 and an F1 score of ≈ 0.49 . Finally, with the *RandF Classifier* we get the best results of ≈ 0.93 for the accuracy and ≈ 0.94 for the F1 score.

Background on Random Forest. The URANUS framework adopts the *Random Forest* algorithm for the classification and regression tasks. Random Forest is an ensemble supervised machine learning technique built by using a combination of tree predictors. The classification is the outcome of a decision taken via a large number of classifiers together. In the Random Forest, each classifier is a Decision Tree (DT) [33] where each tree depends on the values of an independent random vector, and all the trees in the forest have the same distribution. The training algorithm applies the bagging or bootstrap aggregating technique to improve its accuracy and address the overfitting problem. The dataset is created by using the sampling with replacement technique, i.e., some data samples are picked multiple times. The average of the output from the different trees is adopted to predict the behaviour of phenomena. The training phase has been executed by adopting a K-fold cross-validation with $k = 5$.

4.6. Implementation Details

In this section, we provide a thorough description of the implementation details of URANUS. With reference to Figure 4, the following steps are executed:

1. **Step 1. Data Analysis:** In this pre-processing phase, we extract *heatmaps*, *histograms*, and *percentage lists* as described in Section 4.4 for all the entire datasets.
2. **Step 2. Outliers Removal:** In this step, we remove outliers from the Arcus dataset. We replace the values that deviate significantly from the rest of the data by leveraging the Inter Quartile Range (IQR) technique as described in 4.4.

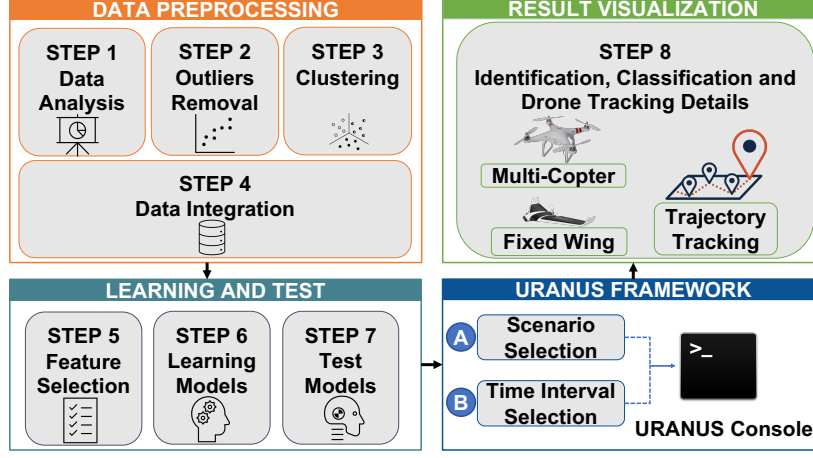


Figure 4: The URANUS Framework workflow.

3. **Step 3. Clustering:** Here, we apply the *k-means* clustering method to the Alvira dataset to classify and extract only the observations related to the drone. We repeat this process in all training scenarios. Finally, to cross-compare the best-fit clustering algorithm, we used the the Silhouette Coefficient as in Eq. 1.

$$S_c = \frac{(b - a)}{\max(a, b)}, \quad (1)$$

where a represent the average intra-cluster distance, and b is the average inter-cluster distance. The value ranges from -1 to 1 . The higher the S_c , the better the specific clustering algorithm fits the experimental data. In our experiments, *k-means* achieves a score of 0.96 compared to 0.88 for Gaussian Mixture Models (GMM), and 0.85 for Agglomerative clustering.

4. **Step 4. Data Integration:** In this step, we merge the datasets from the four sensors (Alvira, Arcus, Diana, and Venus) for each training scenario. We then obtain one large dataset for each training scenario that contains all the readings from the four sensors. Further, we integrate also the *log-files* of the drone(s) during the flight. It is worth noticing that we select the *timestamp* as a reference feature to verify the dataset consistency between the sensor detection and the flying drone(s). We repeat this process for

all the training scenarios.

5. **Step 5. Feature selection:** In this step, we performed a feature selection by using the one-way ANOVA tool as described in Section 4.4. We identified the most highly correlated sensors' features with the drone target variables such as latitude, longitude, speed, altitude, and drone type.
6. **Step 6. Learning Models:** In this phase, we train five machine learning models, one for each target variable. We trained the model by leveraging the Random Forest as a regressor to predict the drone latitude, longitude, speed, and altitude features, and as a classification model to classify the drone type. At the end of the learning process, we obtain five prediction models.
7. **Step 7. Test Models:** We repeat the steps from 1 to 5 for all test datasets. For each scenario, we obtain a dataset containing the data from the four sensors. Then, we use the five prediction models described in step 6 to predict the target variables that are present in all test scenarios.
8. **Step 8. Result Visualization:** In this step, we propose a user interface to select (i) a reference scenario and, (ii) a time interval to perform the drone detection, classification and tracking operations. Based on the time interval, the results are summarized as follows:
 - A time-based drone detection table characterized by parameters such as sensor ID, drone latitude, drone longitude, drone altitude, drone speed, and drone type;
 - A projection of the drone's trajectory (GPS coordinates);
 - Information related to the drone model, and its classification accuracy.

Algorithm 1 summarizes the above-described procedure through pseudo-code.

Input: train_data;
test_scen;
Result: test_prediction;

```

1  // step 1
2  for each scen: do
3      for each sens in scen: do
4          <sens>.data_analysis(train_data);
5          <sens>_clean_data_<scen>=<sens>.clean_data(train_data);
6          // step 2
7          if sens == 'Arcus' then
8              | arcus_clean_data_<scen>=clean_arcus_outliers(scen);
9          end
10         if sens == 'Alvira' then
11             | // step 3
12             | alvira_clust_<scen>=alvira_clust(scen);
13         end
14     end
15 for each scenario: do
16     // step 4
17     merge_<scen>=merge([alvira_clust_<scen>,
18         arcus_clean_data_<scen>, diana_clean_data_<scen>,
19         venus_clean_data_<scen>, drone_<scen>]);
20     // step 5
21     best_feat_<scen>=anova_feat_sel(merge_<scen>);
22     // step 6
23     model_<feat>=train_mod_<feat>(merge_<scen>, best_feat_<scen>);
24 end
25 models=[model_lat, model_long, model_alt, model_speed,
26     model_drone_type]; // step 7
27 test_dataset=get_sens_test_data(test_scen);
28 test_prediction=start_prediction(test_dataset, models); // step 8
29 start_console(test_prediction);

```

Algorithm 1: Pseudo-code of URANUS.

5. Results and Discussions

In this section, we present and discuss the results of the drone identification classification and tracking system. We discuss the metrics for evaluating machine learning models for both regression and classification modelling in Section 5.1, while in Section 5.2 we analyse the performance of the model.

5.1. Metrics Evaluations

In this section, we describe the regression and classification metrics adopted for the URANUS evaluation. We adopted the Mean Squared Error, Mean Absolute Error, and the R-Squared (R^2) metrics to evaluate the model performance and the prediction error rates in regression analysis. Let n be the number of observations in the dataset on all variables, y_i represents the observed values of the variable being predicted, \hat{y}_i defines the predicted values and \bar{y}_i is the mean value of \hat{y}_i . The MSE defined in Eq. 2 and the MAE defined in Eq. 3 represent the difference between the original and predicted data extracted by averaged (for the MAE) or squared (for the MSE) the absolute difference over the dataset. The lower the MAE and MSE, the better the model fits the dataset. Finally, the coefficient R^2 defined in Eq. 4 measures how well the values fit compared to the original data. The coefficient can assume values in the range of $[0, \dots, 1]$. The higher the value for R^2 , the better the performance.

$$MSE = \frac{1}{n} \sum_{i=1}^n (y_i - \hat{y}_i)^2 \quad (2)$$

$$MAE = \frac{1}{n} \sum_{i=1}^n |y_i - \hat{y}_i| \quad (3)$$

$$R^2 = 1 - \frac{\sum (y_i - \hat{y}_i)^2}{\sum (y_i - \bar{y}_i)^2} \quad (4)$$

To evaluate the classification model performance, we used accuracy, precision, recall and F1 score metrics. Let TP represents the True Positive, TN the True Negative, FP the False Positive and FN the False Negative. The accuracy defined in Eq. 5 is the ratio of correctly predicted observations to the total observations, and it describes how the model performs across all classes. The

higher the value, the better the performance of the model. The precision defined in Eq. 6 represents the ratio of correctly predicted positive observations to the total predicted positive observations. This metric measures the reliability of the model in classifying a sample as positive. The recall (known also as sensitivity) shown in Eq. 7 is the ratio between the number of positive samples correctly classified as positive to all observations in the actual class. The recall measures the ability of the model to detect positive observations. The higher the recall, the more positive observations are detected. Finally, F1 score in Eq. 8 is the weighted average of precision and recall. It reaches the maximum value of 1 only if precision and recall are both at 100%. Overall, the F1 score is a metric for comparing different models predicting the same variable.

$$Accuracy = \frac{TP + TN}{TP + TN + FP + FN} \quad (5)$$

$$Precision = \frac{TP}{TP + FP} \quad (6)$$

$$Recall = \frac{TP}{TP + FN} \quad (7)$$

$$F1 = 2 \cdot \frac{Recall \cdot Precision}{Recall + Precision} \quad (8)$$

5.2. Model Evaluation

In this section, we provide the results of our analysis by reporting the experimental results. To investigate the effectiveness of the Random Forest regressor and classifier, we computed the metrics mentioned in Section 5.1 to the target features model such as drone latitude, longitude, speed and altitude in Table 5, and drone type in Table 6 for all the training scenarios reported in Table 4.

- **Latitude:** In each scenario, the metric R^2 provides good results. In particular, the lowest value is 0.7060 for the *Scenario 3.Parrot.a*, while the highest value is 0.9800 for the *Scenario 1.1*. The MAE shows that we have the highest error of 0.0006 *Scenario 3.Parrot.a*, while we have the optimal value of 0.0001 in *Scenario 2.2*. Moreover, for the MSE, we observe that we have the highest error of 0.0032 in *Scenario 3.Parrot.a*, while the lowest of 0.0001 in *Scenario 1.1*. This analysis helped us to

Table 5: Results of the metrics used to measure the performance of the Random Forest models in the form of a *regressor*, on the features Latitude, Longitude, Speed, and Altitude in the various *training* scenarios.

Feature	Metrics	Scenario 1.1	Scenario 1.2.b	Scenario 1.3	Scenario 1.4	Scenario 2.1	Scenario 2.2	Scenario 3.Parrot.a
Latitude	R^2	0.9800	0.8820	0.8460	0.9460	0.8540	0.9420	0.7060
	MAE	0.0003	0.0003	0.0003	0.0002	0.0003	0.0001	0.0006
	MSE	0.0001	0.0010	0.0007	0.0004	0.0007	0.0002	0.0032
Longitude	R^2	0.9800	0.8760	0.8440	0.7460	0.8400	0.9420	0.6980
	MAE	0.0001	0.0009	0.0008	0.0005	0.0009	0.0004	0.0018
	MSE	0.0003	0.0026	0.0019	0.0010	0.0012	0.0011	0.0035
Speed	R^2	0.7900	0.8700	0.8680	0.8480	0.8460	0.8920	0.5760
	MAE	0.1051	1.0432	0.4040	0.7480	1.2620	0.5540	1.1214
	MSE	0.3484	1.9718	1.0300	1.7520	2.3240	1.2720	2.0220
Altitude	R^2	0.8400	0.8320	0.8920	0.9320	0.9800	0.8800	0.8880
	MAE	0.5640	0.6160	0.2400	1.7120	0.3500	0.6360	2.3180
	MSE	2.3760	2.3000	0.8340	4.2320	1.3880	2.6080	5.1380

identify how our model is less accurate for the *Scenario 3.Parrot.a* than the other scenarios. This outcome is justified given the small amount of data in the provided training dataset.

- **Longitude:** The accuracy of the model is the lower in the *Scenario 3.Parrot.a* for the same reasons as described above, where we have R^2 , MAE, and MSE values of 0.6980, 0.0018 and 0.0035, respectively. The model performs better in *Scenario 1.1* and *Scenario 2.2*, where in the latter we obtain R^2 , MAE, and MSE values of 0.9420, 0.0004 and 0.0011, respectively.
- **Speed:** The errors reported by the MAE and MSE metrics are expressed in meter per second *mps*. We obtain good results in *Scenario 2.2* and *Scenario 1.2.b*, where the R^2 MAE and MSE values are 0.8920, 0.5540 and 1.2720, respectively. The model is less accurate in the *Scenario 3.Parrot.a* where we have values of 0.5760, 1.1214 and 2.0220 for R^2 , MAE and MSE, respectively. For MAE, the maximum value of the mean error is $4km/h$ for *Scenario 2.1*, and the minimum error is $0.36km/h$.

- **Altitude:** In *Scenario 1.1* and *Scenario 1.2*, we have a R^2 coefficient of 0.8400 and 0.83, respectively. The MAE and MSE errors are 0.2400 and 0.8340 in Scenario 1.3. In *Scenario 3.Parrot.a* they are 2.3180 and 5.1380 resulting in poor performance.

The aforementioned models adopted for URANUS for tracking purposes are tested and trained for all the scenarios, with an average of MAE=0.3650, MSE=0.9254 and $R^2 = 0.7502$.

We also evaluated the performance of the Random Forest classifier for the drone type feature to classify drones. Overall, most of the metrics have a value higher than 0.9 which means that the classifier has a good performance to discriminate the drone type. Only in the Mavic Pro case, the classifier’s accuracy and precision concerning the Mavic Pro drone are below 0.77, but still an acceptable performance. We summarize the metric results in Table 6. As shown

Table 6: Analysis of the results of the feature drone type with the Random Forest classifier to the training scenarios.

Metrics	Mavic 2	Mavic Pro	Phantom 4 Pro	Parrot
Accuracy	0.948	0.77	0.952	0.95
Precision	0.952	0.77	0.954	0.95
Recall	0.948	0.95	0.954	0.95
F1	0.944	0.948	0.95	0.95
AUC	0.9	0.914	0.912	0.93

in the confusion matrix in Figure 5, our drone classification task reports the 93.4 of accuracy, with a $TPR = \frac{TP}{TP+FN}$ of 0.97 and $FPR = \frac{FP}{FP+TN}$ of 0.90.

Finally, Figure 6 shows the Receiver Operating Characteristics (ROC) curve associated with the performance of URANUS for classification and identification. It summarized the trade-off between the true positive rate (TPR) and the false positive rate (FPR) by considering the drone type feature. Further more, as additional feature to evaluate the classification model’s performance, we consider the Area Under the Curve (AUC). Indeed, for the four curves AUC

Output Class	Mavic 2	423 23.0%	16 0.9%	2 0.1%	19 1.0%	92.0% 8.0%
	Mavic Pro	5 0.3%	447 24.3%	1 0.1%	7 0.4%	97.2% 2.8%
	Parrot	3 0.2%	17 0.9%	412 22.4%	27 1.5%	89.8% 10.2%
	Phantom 4 Pro	7 0.4%	15 0.8%	2 0.1%	436 23.7%	94.8% 5.2%
		96.6% 3.4%	90.3% 9.7%	98.8% 1.2%	89.2% 10.8%	93.4% 6.6%
		Target Class				
		Mavic 2	Mavic Pro	Parrot	Phantom 4 Pro	

Figure 5: Confusion Matrix for Random Forest Classification model for drone type identification.

spans from 0.9 up to 0.93 (near to the 1) which means an optimal result for the classification model. The blue, red, green and black circles represent the optimal operating points for Mavic Pro, Mavic 2, Parrot, Phantom Pro 4 respectively. In particular, the optimal operating point for Mavic Pro is $FP = 0.037$ and $TP = 0.9729$, while for Mavic 2 is $FP = 0.135$ and $TP = 0.960$, while for Parrot is $FP = 0.0145$ and $TP = 0.9901$, and finally for Phantom Pro 4 is $FP = 0.0467$ and $TP = 0.9666$.

6. Conclusion and Future Work

In this paper, we proposed URANUS, a solution to prevent and detect any unauthorized drone in critical infrastructures. URANUS enjoys several key properties: (i) performs drone identification, (ii) drone classification and (iii) drone tracking of one or more drones in flight—a key feature to carry out any type of drone attack. URANUS also recognizes fixed-wing drones and multi-

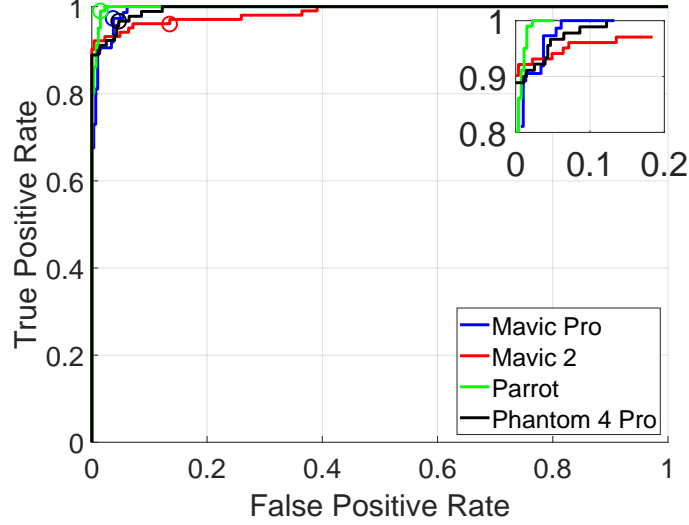


Figure 6: Receiver Operating Characteristics (ROC) curve associated with the detection performance of URANUS. Circles represent the cutoff points, i.e. the optimal operating points.

copter drones via a pure-software machine learning algorithm, based on evaluating error patterns within the trained model. URANUS can be flexibly configured to increase robustness, by using RF/DF and kinematics sensors.

Our experimental performance assessment showed that the Random Forest classifier can achieve 93.4% classification accuracy with a True Positive Rate of ≈ 0.97 and a False Positive Rate of 0.90 computed over a real dataset provided by NATO [10]. The tracking performance achieves an accuracy with an average of $MAE=0.3650$, $MSE=0.9254$ and $R^2 = 0.7502$. Further, for the classification and identification of the drones, the optimal operating point for Mavic Pro is $FP = 0.037$ and $TP = 0.9729$, while for Mavic 2 is $FP = 0.135$ and $TP = 0.960$, while for Parrot is $FP = 0.0145$ and $TP = 0.9901$, and finally for Phantom Pro 4 is $FP = 0.0467$ and $TP = 0.9666$. We also released the source code of URANUS [11], to enable practitioners, industry, and academia, to independently validate our findings and to use our solution as a ready-to-use basis for further investigations. Future work includes the extension of URANUS with capabilities

to identify, classify, and track drones with better accuracy by leveraging state-of-the-art deep learning approaches, in a way to enhance the protection of critical infrastructures.

Acknowledgments

We would like to acknowledge the use of “Drone Detection” dataset provided by NATO Communications & Information Agency (NCIA). The findings reported here are solely responsibility of the authors. The authors would like to thank Giuseppe De Marzo for his help in running the experiments. This work was partially funded by the Italian MISE FSC 2014/20 Asse I project ‘Casa delle Tecnologie Emergenti’, and by the Italian P.O. Puglia FESR 2014/20 project 6ESURE5 ‘Secure Safe Apulia’.

References

- [1] Y. Inoue, Satellite-and drone-based remote sensing of crops and soils for smart farming—a review, *Soil Science and Plant Nutrition* 66 (2020) 798–810.
- [2] F. A. Almalki, B. O. Soufiene, S. H. Alsamhi, H. Sakli, A low-cost platform for environmental smart farming monitoring system based on iot and uavs, *Sustainability* 13 (2021) 5908.
- [3] Y. Inoue, M. Yokoyama, Drone-based optical, thermal, and 3d sensing for diagnostic information in smart farming—systems and algorithms—, in: *IGARSS 2019-2019 IEEE International Geoscience and Remote Sensing Symposium*, IEEE, 2019, pp. 7266–7269.
- [4] A. Mukherjee, P. Mukherjee, D. De, N. Dey, igridedgedrone: Hybrid mobility aware intelligent load forecasting by edge enabled internet of drone things for smart grid networks, *International Journal of Parallel Programming* 49 (2021) 285–325.

- [5] T. J. Aransiola, V. Ceccato, The role of modern technology in rural situational crime prevention: A review of the literature, *Rural Crime Prevention-Theory, Tactics and Techniques* (2020) 58–72.
- [6] T. E. A. Barton, M. Azhar, Open source forensics for a multi-platform drone system, in: *International Conference on Digital Forensics and Cyber Crime*, Springer, 2017, pp. 83–96.
- [7] S. H. Alsamhi, O. Ma, M. S. Ansari, S. K. Gupta, Collaboration of drone and internet of public safety things in smart cities: An overview of qos and network performance optimization, *Drones* 3 (2019) 13.
- [8] R. Di Pietro, G. Oligeri, P. Tedeschi, JAM-ME: Exploiting Jamming to Accomplish Drone Mission, in: *2019 IEEE Conference on Communications and Network Security (CNS)*, 2019, pp. 1–9.
- [9] P. Tedeschi, S. Sciancalepore, R. Di Pietro, PPCA - Privacy-Preserving Collision Avoidance for Autonomous Unmanned Aerial Vehicles, *IEEE Transactions on Dependable and Secure Computing* (2022) 1–1.
- [10] N. A. T. O. (NATO), Drone detection - class i unmanned aircraft systems (uas) tracking, classification and identification challenge, *Kaggle* (????).
- [11] Giuseppe De Marzo, Domenico Lofù, Pietro Tedeschi, Source code of URANUS, <https://github.com/domenicolofu/uranus/>, 2022.
- [12] M. F. Al-Sa'd, A. Al-Ali, A. Mohamed, T. Khattab, A. Erbad, RF-based drone detection and identification using deep learning approaches: An initiative towards a large open source drone database, *Future Generation Computer Systems* 100 (2019) 86–97.
- [13] S. Basak, S. Rajendran, S. Pollin, B. Scheers, Combined RF-Based Drone Detection and Classification, *IEEE Transactions on Cognitive Communications and Networking* 8 (2022) 111–120.

- [14] S. Al-Emadi, F. Al-Senaid, Drone Detection Approach Based on Radio-Frequency Using Convolutional Neural Network, in: 2020 IEEE International Conference on Informatics, IoT, and Enabling Technologies (ICIOT), 2020, pp. 29–34.
- [15] M. S. Allahham, T. Khattab, A. Mohamed, Deep Learning for RF-Based Drone Detection and Identification: A Multi-Channel 1-D Convolutional Neural Networks Approach, in: 2020 IEEE International Conference on Informatics, IoT, and Enabling Technologies (ICIOT), 2020, pp. 112–117.
- [16] O. O. Medaiyese, A. Syed, A. P. Lauf, Machine Learning Framework for RF-Based Drone Detection and Identification System, in: 2021 2nd International Conference On Smart Cities, Automation & Intelligent Computing Systems (ICON-SONICS), 2021, pp. 58–64.
- [17] B. Sazdić-Jotić, I. Pokrajac, J. Bajčetić, B. Bondžulić, D. Obradović, Single and multiple drones detection and identification using RF based deep learning algorithm, *Expert Systems with Applications* 187 (2022) 115928.
- [18] S. Basak, S. Rajendran, S. Pollin, B. Scheers, Drone classification from RF fingerprints using deep residual nets, in: 2021 International Conference on COMMunication Systems NETWORKS (COMSNETS), 2021, pp. 548–555.
- [19] I. Nemer, T. Sheltami, I. Ahmad, A. U.-H. Yasar, M. A. R. Abdeen, RF-Based UAV Detection and Identification Using Hierarchical Learning Approach, *Sensors* 21 (2021).
- [20] W. Nie, Z.-C. Han, M. Zhou, L.-B. Xie, Q. Jiang, UAV Detection and Identification Based on WiFi Signal and RF Fingerprint, *IEEE Sensors Journal* 21 (2021) 13540–13550.
- [21] M. S. Allahham, M. F. Al-Sa’d, A. Al-Ali, A. Mohamed, T. Khattab, A. Erbad, Dronerf dataset: A dataset of drones for rf-based detection, classification and identification, *Data in brief* 26 (2019) 104313.

- [22] Federal Aviation Administration, No Drone Zone, https://www.faa.gov/uas/resources/community_engagement/no_drone_zone/, 2021. (Accessed: 2022-05-21).
- [23] P. Tedeschi, S. Sciancalepore, R. Di Pietro, ARID: Anonymous Remote IDentification of Unmanned Aerial Vehicles, in: Annual Computer Security Applications Conference (ACSAC), Association for Computing Machinery, 2021.
- [24] R. J. Little, D. B. Rubin, Statistical analysis with missing data, volume 793, John Wiley & Sons, 2019.
- [25] A. W. King, R. Eckersley, Statistics for biomedical engineers and scientists: How to visualize and analyze data, Academic Press, 2019.
- [26] P. Cohen, S. G. West, L. S. Aiken, Applied multiple regression/correlation analysis for the behavioral sciences, Psychology press, 2014.
- [27] L. Bottou, V. Vapnik, Local learning algorithms, Neural computation 4 (1992) 888–900.
- [28] B. T. Polyak, A. B. Juditsky, Acceleration of stochastic approximation by averaging, SIAM journal on control and optimization 30 (1992) 838–855.
- [29] A. Beygelzimer, E. Hazan, S. Kale, H. Luo, Online gradient boosting, Advances in neural information processing systems 28 (2015).
- [30] G. Biau, E. Scornet, A random forest guided tour, Test 25 (2016) 197–227.
- [31] S. R. Gunn, et al., Support vector machines for classification and regression, ISIS technical report 14 (1998) 5–16.
- [32] E. Zanyaty, Support vector machines (svms) versus multilayer perception (mlp) in data classification, Egyptian Informatics Journal 13 (2012) 177–183.
- [33] L. Breiman, Bagging predictors, Machine learning 24 (1996) 123–140.